Progress in research and education project in collaboration with UEC

Hiroshi Hirai*

（Received January 7, 2019）

1. Introduction

In March 2018, I launched a cooperative research project with the University of Electro-Communications (UEC). Its purpose is not only to gain access to experimental equipment at the UEC, but also to engage in discussions with academic staff and graduate students. Here, I report the current status of this project and its future direction.

2. The University of Electro-Communications

The UEC is a national university located in Chofu in Tokyo Metropolis. Figure 1 shows the front gate of the UEC. Chofu is located almost at the center of Tokyo Metropolis, in the southeastern part of Tama District, and 15 km from Shinjuku. This area is served by the Keio Line, running east-west, National Highway 20, and the Chuo Expressway. The UEC is about five minutes walk from Chofu station on the Keio Line.

Fig.1. Front gate of UEC

The UEC was originally the Technical Institute for Wireless Communications, which was founded by the Wireless Association in 1918. It was then transferred to the Ministry of Communications in 1942. Finally, it was transferred to the Ministry of Education and set up as a national university in 1949.

The UEC consists of a faculty and a graduate school. The faculty of Informatics and Engineering consists of three Clusters: Cluster I (Informatics and Computer Engineering), Cluster II (Emerging Multi-interdisciplinary Engineering), Cluster III (Fundamental Science and Engineering). In Cluster I, the students learn the fundamentals of information science. In Cluster II, they learn the fundamentals to study the new academic field by fusion of information science and engineering. In Cluster III, they explore the creation of materials and devices with completely new functions and study the origin of their characteristics. The faculty has about three thousand students.

The educational policy of the faculty is to cultivate a wide range of fundamental capabilities and the level of expertise required to support an advanced communication society. The overall goals are to provide students with the ability to think scientifically on a wide range of topics, to cultivate scientific and engineering ethics and social and international awareness, and to master logical communication skills.

Many graduating students go on to graduate school to carry out more advanced studies and research. The resulting human resources are highly valued in various fields because they have acquired advanced professional skills, a broad education and an international frame of mind.

The Graduate School of Informatics and Engineering consists of the Department of Informatics, the Department of Communication Engineering and Informatics, the Department of Mechanical Engineering and Intelligent Systems and the Department of Engineering Science. The number of graduate students is about a thousand.

I am collaborating with Dr. H. Shimada, who belongs to the Department of Engineering Science, and is a full-time academic staff member in charge of education in Cluster III. In his laboratory, he supervises about ten students in their research, which is mainly related to small Josephson junctions. In order to clarify the relation between his research and mine, I provide an outline of his studies below.

*Department of Electronic Media Technology

Generally, when tunnel junctions are made very small, the effect of the charge associated with a single electron can be significant. If the electrostatic potential on both sides of the junction is initially the same, tunneling of a single electron will introduce a charge of +*e* and -*e* on either side. The electrostatic energy in this situation is $E_C = e^2/2C$, where C is the capacitance. When the area of the junction is reduced to less than about 0.1 µm × 0.1 µm, E_C will be as large as 1 K in terms of thermal energy. This has a large effect on the tunneling behavior at cryogenic temperatures. Studies on single electron charging effects are often carried out using devices with more than two tunnel junctions. The most typical device is a single electron tunneling (SET) transistor.

Such SET transistors can be either metal- or semiconductor-based. In a metal-based SET transistor a Coulomb island, separated from leads (source and drain electrodes), is formed by two small tunnel junctions, and a gate electrode is placed beside it. Aluminum is often used, since the surface aluminum oxide film is a very good insulator for forming a tunnel junction. Aluminum becomes a superconductor at low temperature, and a superconducting SET transistor is typically composed of two small Josephson junctions. It is an interesting system in which the Josephson effect and the single electron charging effect compete with each other. These types of Josephson junctions are used in the quantum computers currently being studied globally.

Such devices are typically fabricated using a process involving photoresist deposition, electron beam lithography and metal deposition in a vacuum. All of the equipment required for this fabrication process is available either in Dr. Shimada's laboratory or in shared facilities at the UEC. To investigate the weak Josephson effect, it is necessary to measure the electrical resistance at temperatures of less than 1 K using liquid helium. Fortunately, a helium gas liquefier is available at the UEC, so that liquid helium can be obtained very inexpensively. Dr. Shimada's laboratory also contains several dilution refrigerators, which are required for experiments at such low temperatures. Therefore, all processes from device fabrication to low-temperature measurements can be performed in a single location.

3. Transporting equipment and setting it up

In March 2018, I loaded equipment including a cryostat, a sample holder, and an XY recorder at the National Institute of Technology, Gunma College (NITGC) onto a light truck and transported it to the UEC.   The route was along the Kanetsu Expressway, Sasame dori, Ring Road No.8 and the Koshu Highway, and took about 2.5 hours. The cryostat had been disassembled at NITGC into components including two glass dewars, a superconducting magnet, and a metal flange, and these were reassembled at the UEC.

In August 2018, I set up the laboratory at the UEC, as shown in Fig. 2. First, the cryostat was connected to a helium gas recovery system. It consists mainly of a rotary pump, a three-way valve, two leak valves, two additional valves, a vacuum gauge, and a helium gas purity meter. The handles for the three-way valve and leak valve 2 can be seen on the yellow plate in the figure.

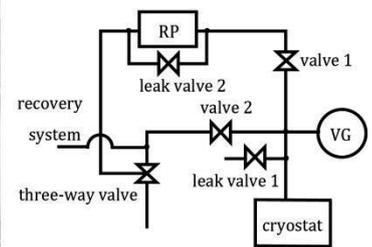Fig. 2. Helium gas recovery system

Fig. 3. Schematic drawing of helium gas recovery system

Figure 3 shows a schematic diagram of the recovery system. If valve 1 is closed and valve 2 is opened, the cryostat is connected to the recovery system. If valve 2 is closed, and valve 1 is opened, and the three-way valve is connected to the side of the recovery system, the cryostat can be pumped by the rotary pump and helium gas can be sent to the recovery system.

Figure 4 shows the rack carrying the instruments for measuring the magnetoresistance. From the top, these are an NF 5610B lock-in amplifier, a Lake Shore 647 magnet power supply, and a Yokogawa 3022 XY recorder. The current flowing in the superconducting magnet can be determined based on the output voltage of the magnet power supply, which is proportional to the current. This voltage was input to the X terminal of the XY recorder. Lock-in detection was used to measure the voltage in order to determine the electrical resistance. This was performed using a lock-in amplifier and an NF LI-75A differential preamplifier. The measured voltage was input to the Y terminal of the XY recorder.

Fig.4. Rack with measurement equipment

In September 2018, I performed an experiment using liquid helium to measure the magnetoresistance of a GaAs/AlGaAs epitaxial wafer formed into a Hall-bar shape using photolithography and wet etching. As shown in Fig. 5, a two-dimensional electron gas is generated at the interface in the heterostructure.
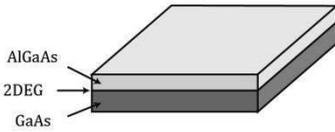

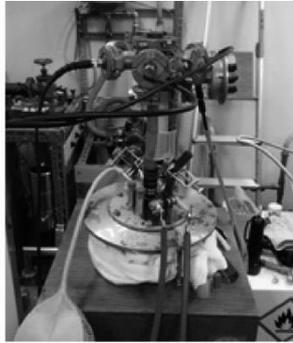Fig.5. AlGaAs/GaAs heterostructure   Fig. 6. Sample holder

The sample was mounted on a sample holder, which was inserted into a cryostat cooled to 4.2 K, which is the boiling point of liquid helium. As shown in Fig. 6, frost formed on the metal flange at the top of the cryostat at this low temperature. The two thick red lead wires provided electrical current to the superconducting magnet. Black BNC cables for supplying current to the sample were connected to each terminal at the top of the sample holder. The orange balloon seen at the bottom left of Fig. 6 was designed to rupture and ensure safety if the pressure inside the cryostat rose suddenly due to quenching of the superconducting magnet.

The magnetoresistance in a two-dimensional electron gas can be qualitatively explained as follows. The kinetic energy of the two-dimensional electron gas in an applied magnetic field is given by the Hamiltonian, $H =$

$\frac{1}{2m^*}\left(\vec{p} + e\vec{A}\right)^2$, where m^* is the effective mass of the conduction electrons, and $\vec{p}$ is their momentum vector. The Landau gauge $\vec{A} = (0, Bx)$ is used for the vector potential corresponding to a uniform magnetic field in the z direction, where B is the magnitude of the magnetic field. Based on elementary quantum mechanics, this Hamiltonian formally describes a one-dimensional harmonic oscillator, and its energy is quantized into the Landau levels, $\varepsilon(N) = \hbar\omega_c\left(N + \frac{1}{2}\right)$ $(N = 0, 1, \cdots)$. Here, $\omega_c = eB/m^*$ is the cyclotron angular frequency, N is the Landau quantum number, e is the elementary charge of an electron, and $\hbar = h/2\pi$ is the reduced Planck constant. The orbital motion for a Landau quantum number N classically corresponds to cyclotron circular motion with a radius $(2N + 1)^{1/2}l_B$. Here, $l_B = (\hbar/eB)^{1/2}$ is referred to as the magnetic length, and equals 8.11 nm for $B = 10$ T. The quantum states $eB/h = 1/2\pi l_B^2$ per unit area are degenerate for each Landau level, which corresponds to the fact that the energies are the same regardless of the center coordinates of the cyclotron circular motion.

Since the electrostatic potential randomly fluctuates in a real system, the density of states for each Landau level has a non-zero width Γ. This is due to the fact that because of the fluctuating potential, the degeneracy regarding the center coordinates of the cyclotron circular motion partly disappears. That is, the energy associated with cyclotron circular motion with center coordinates in the vicinity of the peak of the electrostatic potential becomes higher than the average value. Since electrons are scattered and the cyclotron circular motion is disturbed, the quantized levels are blurred to some extent, leading to a non-zero Γ, given by $\Gamma = h/\tau$, where τ is the average scattering time for conduction electrons. In a real electron system, the density of states at the Fermi level shows periodic oscillation with respect to the reciprocal of the magnetic field. A similar oscillation is also observed for the electrical resistance, and this is referred to as the Shubnikov-de Haas effect.

In order to observe the Shubnikov-de Haas effect, the interval between adjacent Landau levels, $\hbar\omega_c$, must be sufficiently larger than Γ. This condition is equivalent to $\omega_c\tau \gg 1$. In a high-mobility two-dimensional electron gas, this condition is satisfied even for relatively low magnetic fields, and quantum oscillations in the magnetoresistance

can be observed as the magnetic field is increased. The amplitude of these oscillations increases with increasing magnetic field, and eventually the minimum value of the oscillating magnetoresistance becomes zero. Under a sufficiently strong magnetic field, the longitudinal resistivity ρ_{xx} becomes zero over an extended magnetic-field range, while the Hall resistivity ρ_{xy} becomes constant, forming a plateau. Moreover, this constant value equals the physical constant, $h/e^2 = 25.81$ kΩ, divided by an integer. In terms of conductivity tensor components, this is expressed as $\sigma_{xx} = 0$, $\sigma_{xy} = i(e^2/h)$, $(i = 1,2,\cdots)$, and is referred to as the integer quantum Hall effect.

Below are my experimental results for the GaAs/AlGaAs heterostructure sample described above. The temperature of the sample was 4.2 K. As can be seen in Fig. 7, Shubnikov-de Haas oscillations are observed in the longitudinal resistivity ρ_{xx}. In addition, plateaus are observed in the Hall resistivity ρ_{xy}. These plateaus are experimental evidence of the integer quantum Hall effect.
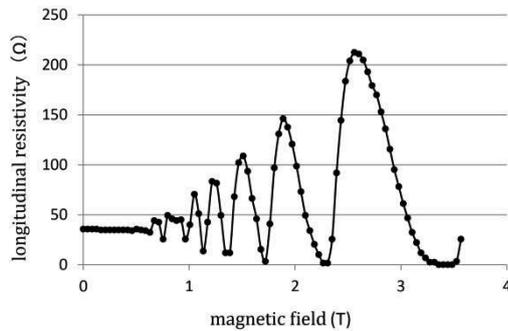

Fig. 7 . Longitudinal resistivity as function of magnetic field

The classical Hall resistivity is given by $\rho_{xy} = B/ne$, where n is the number of conduction electrons per unit area. As described above, since the eigenstates of eB/h per unit area are degenerate for each Landau level, the equation $n = i(eB/h)$ is satisfied when the i-th Landau level is completely filled with electrons. When $i(eB/h)$ is substituted for n, the Hall resistivity becomes $\rho_{xy} = (1/i)(h/e^2)$, and quantization of the Hall resistance can be derived formally. However, this argument only holds when the i-th Landau level is completely filled with electrons. However, a surprising

aspect of the quantum Hall effect is that the Hall resistance remains at its quantized value even when the number density, n, is slightly changed.

In order to understand the plateaus in the Hall resistance, the localization of electrons in a strong magnetic field has to be considered. As described above, Landau level broadening occurs due to random fluctuations in the potential. In a strong magnetic field where the quantum Hall effect is observed, the magnetic length l_B is sufficiently smaller than the characteristic length for the spatial variations of the potential. Therefore, electrons move along the contour lines of the potential fluctuations while undergoing cyclotron circular motion with a radius of about l_B. The high-energy side of the broadened Landau levels corresponds to trajectories in the peak regions of the fluctuating potential, whereas the low-energy side corresponds to trajectories in the valley regions. Both types of trajectories are localized states because they are closed curves surrounding local maxima or minima.

The quantum Hall effect will be observed when the field strength becomes sufficiently high. Only when the Fermi level is in the localized states, the longitudinal conductivity of the sample at low temperature will be $\sigma_{xx} = 0$ and the Hall conductivity will be constant. This is a simplified explanation of the quantum Hall effect.

4.   Future prospects

It is now possible to carry out experiments at low temperature using liquid helium, and fabricate samples using techniques such as photolithography at the UEC. In future work, I would like to attempt to carry out experiments to investigate hot spots in the quantum Hall regime, and the phase coherence of conduction electrons in metallic thin films at low temperature. In addition, I would like the students at NITGC to make use of the experimental facilities at the UEC for their graduation research.

5.   References

(1)   National University Corporation, the University of Electro Communications, "Annai" (2018).
(2)   National University Corporation, the University of Electro Communications, "Gaiyou" (2017 – 2018).